10.1515/astro-2017-0197

Baltic Astronomy, vol. 24, 9–16, 2015

INTERSTELLAR MATTER STRUCTURE ALONG THE LINE OF SIGHT TO CYG X-1

N. G. Bochkarev[1,2], E. A. Karitskaya[3], V. G. Klochkova[4] and M. V. Yushkin[4]

[1] *Sternberg Astronomical Institute of M. V. Lomonosov Moscow State University, Universitetskij prosp. 13, Moscow 119991, Russia; boch@sai.msu.ru*

[2] *Eurasian Astronomical Society, Universitetskij prosp. 13, Moscow 119991, Russia*

[3] *Institute of Astronomy of Russian Academy of Sciences, Pyatnitskaya str. 48, Moscow 119017, Russia; karitsk@yandex.ru*

[4] *Special Astrophysical Observatory of Russian Academy of Sciences, Nizhnij Arkhyz 369167, Russia*

Received: 2014 November 29; accepted: 2014 December 19

Abstract. High-resolution spectra ($R = 60\,000$) of Cyg X-1 = V1357 Cyg obtained with the NES echelle spectrograph of the Russian 6 meter telescope (3950–6690 Å) were used to study narrow interstellar absorption lines. We resolved the interstellar line blends by fitting them with Gaussian profiles. The main three absorption components, with the heliocentric radial velocities $V_r = -1$, -13 and -26 km s^{-1}, were revealed. They correspond to three interstellar gas and dust complexes along the line of sight to the object. Thus, we get information on the distribution of interstellar matter along the way to Cyg X-1. The interstellar calcium abundance and ionization degree, averaged along the line of sight, were determined. A weak component with $V_r = -43$ km s^{-1} is revealed in the profiles of the strongest lines. We relate it to the approaching wall of the expanding interstellar envelope around the Cyg OB3 association (superbubble). This finding supports the view that Cyg X-1 was born in this stellar association and is still located in it.

Key words: ISM: structure – ISM: interstellar lines – stars: X-ray binary: Cyg X-1 – stars: V1357 Cyg – stars: optical spectroscopy

1. INTRODUCTION

Cyg X-1 is an X-ray binary system whose relativistic component is the first black hole candidate discovered. More than 4000 papers on Cyg X-1 have been published. Thus, it is important to know the properties of matter through which the object is observed. For example, this knowledge is important for the interpretation of interstellar scattering of X-rays from Cyg X-1.

The optical component, an O 9.7 Iab supergiant, is responsible for about 95 % of the system's optical luminosity. However, estimates of its absolute X-ray and optical luminosity depend on the distance d to this X-ray binary. The distance was recently determined as $d = 1.8 - 2.0$ kpc from trigonometric radio parallax measurements (Reid et al. 2011). Earlier we suspected a somewhat larger distance

Table 1. Spectroscopic observations of Cyg X-1 with the 6 m telescope.

Dates of observations	$N_{\rm nights}$	$N_{\rm spectra}$	Band, Å
2005 November 12	1	2	4557–6015
2005 November 13–19	2	6	5274–6693
2006 March 14–15	2	7	3978–5462
2006 August 7–15	6	24	4010–5460
2007 July 24 – Sept. 5	7	22	3943–5398
2008 August 17–19	2	7	4548–6005

($d = 2.0-2.3$ kpc), based on interstellar extinction measurements and the location of Cyg X-1 in Cyg OB3 which is at a distance of 2.3 kpc according to the old Galactic scale (Bochkarev & Karitskaya 2007). From a recent determination of distances to OB associations, Cyg OB3 is at a distance of 1.8 kpc (Melnik & Dambis 2009), therefore $d = 1.8$ kpc may be the real distance to Cyg X-1.

An indirect test of the distance estimates can be a determination of the number of interstellar complexes along the way to Cyg X-1 and its comparison to independently observed large-scale inhomogeneities of interstellar matter. With this purpose in mind, the present paper is aimed at a study of interstellar line profiles. We use high-resolution spectra obtained with the 6 m telescope in the frame of our program of long-term spectroscopic monitoring of Cyg X-1 in the optical range (Karitskaya 2003; Karitskaya et al. 2006; Karitskaya et al. 2008).

2. OBSERVATIONS AND REDUCTIONS OF SPECTRA

We obtained spectra of Cyg X-1 with the NES echelle spectrograph in the Nasmyth focus of the 6 m telescope of the Special Astrophysical Observatory of the Russian Academy of Sciences (SAO RAS) (Panchuk et al. 2007, 2009). The observations were performed with a 2048×2048 CCD and an image slicer (Panchuk et al. 2009).

We used a modified ECHELLE context (Yushkin & Klochkova 2005) of the MIDAS package to extract one-dimensional vectors from the two-dimensional echelle spectra. Cosmic ray hits were removed via median averaging of two successively taken spectra. Wavelength calibration was performed using spectra of a hollow-cathode Th-Ar lamp.

During 20 nights in 2005–2008, 68 spectra were obtained. The red region of the optical spectrum was observed in 2005 and 2008, and the blue region, in 2006–2007 (Table 1). The spectral resolution is $R \simeq 60\,000$. The signal-to-noise ratio, S/N, calculated per pixel in 1D spectra is up to 330, which corresponds to $\simeq 500$ per resolution element of $\simeq 4.6$ km s^{-1}.

3. INTERSTELLAR LINES

The spectra reveal the supergiant absorption lines: H I, He I, He II, CNO λ4640Å blend, a lot of other lines of heavy elements (C, N, O, Ne, Mg, Si, S, Fe, Zn), and strong emission components of Hα and He II at 4686 Å lines with complex variable profiles. The spectra also show narrow interstellar absorption lines as well as numerous diffuse interstellar bands (DIBs). In this paper, we study the profiles of narrow lines of atoms, the CH molecule, and their ions only (Table 2). For this purpose, all of the spectra were reduced to heliocentric coordinate system and

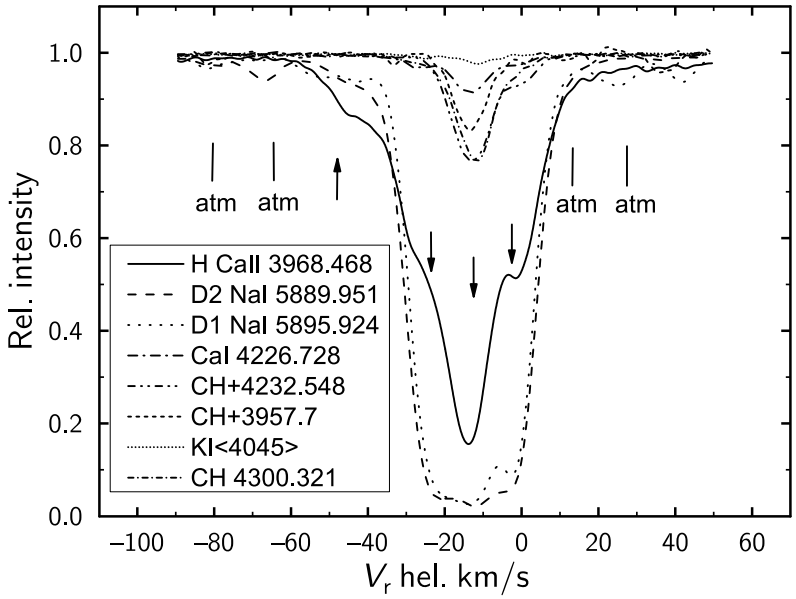

Fig. 1. Profiles of interstellar lines in the optical spectra of Cyg X-1, obtained with the 6 m telescope: relative intensity vs. heliocentric radial velocity $V_{\rm r\,hel}$. The inset identifies curves used for different species. Labels 'atm' mark the positions of the telluric H_2 absorption lines in the D1 and D2 Na I line profiles. Arrows indicate radial velocities of the main components of the interstellar line profile.

summed up. The resulting line profiles are shown in Fig. 1.

The first column of Table 2 contains the wavelengths of the measured interstellar lines. Wavelength <4045> corresponds to the averaged profile of the weak K I 4044, 4047 Å doublet. It was smoothed using a Gaussian filter with a width of 2 km s^{-1}. The second column lists the species forming the lines. For the Ca II line and Na I doublet, Fraunhofer designations are also given. The third column presents numbers of spectra we averaged. The fourth column contains the signal-to-noise ratio, S/N, calculated as the square root of the number of counts in continuum of the summarized spectrum in the lines' neighborhood. The fifth column presents the depth of the spectral lines with respect to continuum. The sixth column gives the radial velocity of the deepest parts of the spectral lines. The next three columns contain the line widths, in km s^{-1}, respectively at the levels of 0.25, 0.5 and 0.75 of the line depth. The tenth column gives the equivalent width of the line, in mÅ. References to remarks are collected in the last column.

Depressions seen within the spectrum fragments containing the D1 and D2 Na I line profiles, marked in Fig. 1 with labels 'atm', are telluric absorption lines of molecular hydrogen we have not removed. Pollution with telluric lines occurs only in the red part of the spectrum and, within the displayed spectrum fragments, its depth does not exceed 5% of the relative intensity of stellar continuum. Fortunately, the telluric lines overlapping the interstellar absorption lines are weak enough and create distortion of their profiles which does not exceed 2%. A weak telluric line occurs in the central part of the D2 Na I line profile around $V_{\rm r} = -16$ km s^{-1} and distorts it by about 2%.

Table 2. Interstellar lines in the optical spectra of Cyg X-1.

λ (Å)	Species	$N_{\rm spectra}$	S/N	Line depth	$V_{\rm r}$ (km s^{-1})	$\Delta V_{0.25}$ (km s^{-1})	$\Delta V_{0.5}$ (km s^{-1})	$\Delta V_{0.75}$ (km s^{-1})	W_λ, (mÅ)	Rem.
3957.7	CH^+	22	150	0.166	–13.3	6.7	10.3	15.2	34	1
3968.468	H Ca II	22	170	0.843	–13.8	5.9	30.4	41.8	354	
4044.136	K I	53	200	0.027	–11.5	5	21	22	4.8	
4047.206	K I	53	200	0.014	–10.7	6	15	33	2.5	
<4045>	K I	53	250	0.021	–11.3	4.7	10	24	4.1	2
4226.728	Ca I	53	310	0.084	–13.1	7.2	11.4	30.4	21	
4232.548	CH^+	53	290	0.230	–13.0	8.4	12.8	23.4	52	
4300.321	CH	53	330	0.233	–11.7	7.1	11.1	18.3	45	
5889.951	D2 Na I	15	240	0.980	–12.5	30.1	35.4	41	733	3
5995.924	D1 Na I	15	240	0.978	–14.4	28.8	33.5	38.7	691	3

Remarks. 1: A defect in the spectra, the profile is not very reliable. 2: The summary profile of the K I doublet. 3: The profile is somewhat distorted because of overlap with weak telluric lines in the parts of spectra marked with ticks in Fig. 1.

Using the measured equivalent widths (Table 2), the calcium abundance along the way to Cyg X-1 can be determined. The interstellar extinction $A_V = 3.36$ mag (Walborn 1973) means that the hydrogen column density is $N(\mathrm{H}) = 7 \cdot 10^{21}$ cm^{-2}. The equivalent widths of Ca I 4226 Å and Ca II 3968 Å spectral lines (Table 2) correspond to the Ca I and Ca II column densities $N\,(\mathrm{Ca\,I}) = 0.8{\cdot}10^{11}$ cm^{-2} and $N\,(\mathrm{Ca\,II}\ 3968\ \text{Å}) = 3.2{\cdot}10^{12}$ cm^{-2}, respectively. The total Ca column density is thus $N(\mathrm{Ca}) = 3.3 \cdot 10^{12}$ cm^{-2} and $N(\mathrm{Ca\,I})/N(\mathrm{Ca}) = 0.024$. This means that the interstellar Ca abundance averaged along the line of sight to Cyg X-1 is $[N(\mathrm{Ca})/N(\mathrm{H})]_{\rm ISM} = 6 \cdot 10^{-10}$. Taking into account that the Ca abundance in the solar atmosphere is $[N(\mathrm{Ca})/N(\mathrm{H})]_\odot = 2 \cdot 10^{-6}$, we have the interstellar Ca depletion $[\mathrm{Ca/H}]_{\rm ISM}/[\mathrm{Ca/H}]_\odot = 3{\cdot}10^{-4}$, typical of interstellar matter in our Galaxy. Unfortunately, only lines of neutral atoms were observed for other elements (Na, K) and it was not possible to find their abundances.

4. STRUCTURE OF INTERSTELLAR MATTER TOWARD CYG X-1

In Fig. 1, the profiles of all interstellar lines that are strong enough reveal three main absorption components, with the heliocentric radial velocities $V_{\rm r} = -1$, -13 and -26 km s^{-1}. These components are considered as absorptions in interstellar gas and dust complexes along the line of sight to the object. Besides, a weak component with $V_{\rm r}$ from -40 to -45 km s^{-1} can be seen. The four components are marked with arrows in the figure.

We resolved interstellar line blends by fitting them with Gaussian profiles through the procedure implemented in the DECH software by Galazutdinov (2007). It can be applied to any kind of spectral data and makes it possible to resolve blended lines, as well as to fit single spectral lines using Gaussian, Lorentzian or Voigt profiles. The results are given in Table 3.

The first column of Table 3 contains the wavelengths of measured interstellar lines. Wavelength <4045> corresponds to the averaged profile of the weak K I 4044, 4047 Å doublet. It was smoothed using a Gaussian filter with a width of 2 km s^{-1}. The second column lists the species forming the lines. The next four columns give the radial velocities $V_{\rm r}$ for the resolved components. The last four columns present the equivalent widths EW of the components, in mÅ. Unfortu-

Table 3. Interstellar line components.

λ (Å)	Species	V_r1 ($km\,s^{-1}$)	V_r2 ($km\,s^{-1}$)	V_r3 ($km\,s^{-1}$)	V_r4 ($km\,s^{-1}$)	$EW1$ (mÅ)	$EW2$ (mÅ)	$EW3$ (mÅ)	$EW4$ (mÅ)
3957.7	CH^+	0.5	–13.2	–	–	4	26	–	–
3968.468	H Ca II	1	–13.9	–27.6	–42	70	169	58	30
<4045>	K I	–	–11	–25.1	–	–	3	1	–
4226.728	Ca I	–1.6	–13.2	–26.1	–	4	12	5	–
4232.548	CH^+	–0.9	–12.8	–32.3	–	7	43	1	–
4300.321	CH	1.5	–12.1	–27.1	–	4	40	3.5	–
5889.951	D2 Na I	–0.2	–14.2	–25.8	–	95	551	57	–
5995.924	D1 Na I	–0.9	–13	–25.2	–43.5	168	302	165	21

nately, a typical uncertainty in EW is about $\pm 50\%$. To improve the accuracy, it is necessary to obtain observations with a higher spectral resolution.

As an example, the resolved Ca II 3968 Å spectral line is shown in Fig. 2. Table 3 and Fig. 2 clearly show that the procedure applied to resolve the components permitted us to reveal the fourth component reliably.

It should be emphasized that the radial velocities in Table 3 and Figs. 1–2 are heliocentric. To find the peculiar velocities of the gas clouds with respect to the local young Galactic objects (interstellar matter and massive stars), a correction for the solar peculiar velocity should be introduced. Following Zabolotskikh et al. (2002) and Melnik & Dambis (2009), we adopted the following solar peculiar velocity components in the Galactic coordinate system: $u_\odot = 10\ km\,s^{-1}$, $v_\odot = 12 \pm 1\ km\,s^{-1}$, $w_\odot = 7 \pm 1\ km\,s^{-1}$. These three values do not depend on the adopted distance R_0 to the center of the Galaxy, at least for the R_0 range $7.0 - 9.0$ kpc (Melnik & Dambis 2009). In this case, the peculiar velocity of the Sun towards Cyg X-1 is $V_{Sun} = 15\ km\,s^{-1}$. For the V_{LSR} velocities of the three main gas and dust complexes with respect to the local standard of rest (LSR), we get about $+14\ km\,s^{-1}$, $+2\ km\,s^{-1}$ and $-7\ km\,s^{-1}$, respectively. These velocities are in sufficiently good agreement with the Galactic rotation component towards Cyg X-1. For the fourth absorption line component, $V_{LSR} \approx -30\ km\,s^{-1}$. The last component may be "genetically" related to the Cyg 3 interstellar loop structure around the Cyg OB3 stellar association (Brand & Zealy 1975; Bochkarev & Sitnik 1985) where the star Cyg X-1 is projected. In addition to the distances to Cyg X-1 and Cyg OB3 being the same ($d = 1.8 - 2.0$ kpc, see Introduction), their proper motions coincide within the errors of measurements. Indeed, for Cyg X-1, the proper motion as measured by *Hipparcos* is: $\mu_\alpha = -0.00382 \pm 0.00079''$; $\mu_\delta = -0.00762 \pm 0.00091''$. According to Melnik & Dambis (2009), the corresponding values for Cyg OB3 are: $\mu_\alpha = -0.0031 \pm 0.00025''$; $\mu_\delta = -0.0071 \pm 0.00025''$. The radial velocities differ somewhat: for Cyg X-1, $V_r = -3.3 \pm 1.1\ km\,s^{-1}$ (Aab 1983), -2 to $-11\ km\,s^{-1}$ (Abubekerov et al. 2004); for Cyg OB3, $V_r = -9.5 \pm 1.8\ km\,s^{-1}$ (Melnik & Dambis 2009). The difference is about $6\ km\,s^{-1}$, within the limits of the velocity dispersion for stars in the Cyg OB3 association ($9.5\ km\,s^{-1}$). Thus, most probably, Cyg OB3 is the birthplace of Cyg X-1 as well as its present location (Ziolkowski 2005; Bochkarev & Kartiskaya 2007). From the above values, we estimate the upper limit on the kick effect for the Cyg X-1 binary to be $16\ km\,s^{-1}$.

The 3D distribution of obscuring interstellar dust in the 2 kpc (in the modern scale, $\simeq 1.6$ kpc) region around the Sun, constructed by Lucke (1978) with a res-

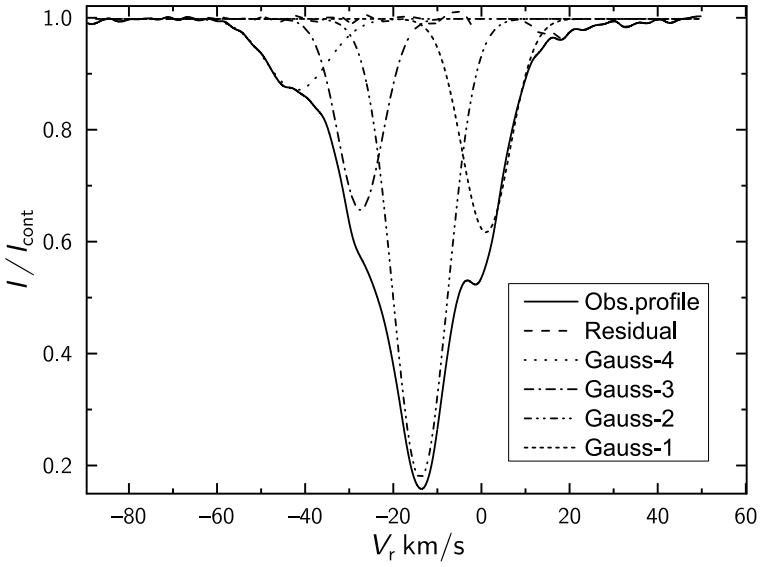

Fig. 2. The resolved interstellar blend of Ca II 3968 Å (solid curve) fitted with four Gaussian profiles vs. the heliocentric radial velocity $V_{\mathrm{r\,hel}}$. The top curve shows the residuals.

olution of 200 pc, indicates three matter condensations (gas and dust complexes) in the direction of Cyg X-1. The nearest (and the weakest) one is located at about 300 pc from the Sun. The second, the largest and highest-density condensation, is associated with the Great Rift dissecting the Milky Way from the constellation Cygnus to the Galactic center and beyond. The edge of obscuring matter in the direction of Cyg X-1, closest to the Sun, is at the distance about 800 pc, the farthest edge being found at about 1300 pc in the old galactic distance scale ($R_0 = 10$ kpc) and at about 1 kpc in the modern one ($R_0 = 7 - 8$ kpc). The third gas and dust complex is located in the Cygnus star formation region, associated with the Cyg OB1, Cyg OB2, Cyg OB3, and Cyg OB8 associations, where Cyg X-1 is located. The nearest edge of the complex is at about 1.5 kpc (for the modern R_0).

We relate the observed three components of the interstellar absorption line profiles (marked with arrows in Fig. 1) to these three gas and dust complexes. The strongest central component with the heliocentric radial velocity $V_{\mathrm{r\,hel}} = -13$ km s^{-1} originates probably in the Great Rift. The other two are probably related to the nearest and the farthest of the complexes. As the line of sight toward Cyg X-1 runs almost along the Local spiral arm, V_{r} is nearly constant along the way to this object: V_{r} variations are comparable to the peculiar velocities of interstellar clouds as well as of OB associations (Melnik & Dambis 2009). Namely, values of V_{r} with respect to the LSR are close to zero. It does not permit us to tell which component is related to the farthest and which one to the nearest complex, though one can expect the line component with the heliocentric velocity -1 km s^{-1} ($V_{\mathrm{LSR}} = +14$ km s^{-1}) to be associated with the farthest gas and dust complex.

The interstellar absorption line profile components at the heliocentric radial

velocity -1 km s^{-1} appear not only in the three strongest lines but also in the lines of CH^+ and Ca I. Line components at the radial velocity -26 km s^{-1} appear in the same lines, but are a bit weaker. The high-velocity, $V_r = -43$ km s^{-1}, components are detectable only in the strongest D1 Na I (unfortunately, this component in the D2 Na I line is blended with a weak telluric line) and H Ca II lines. It may indicate the differences in physical conditions and, probably, in the chemical composition in gas and dust complexes along the line of sight.

5. CONCLUSIONS

From high-resolution spectra of Cyg X-1 = V1357 Cyg ($R = 60\,000$) obtained with the NES echelle spectrograph of the 6 m telescope (SAO RAS), narrow interstellar absorption lines were studied. We resolved the interstellar line blends by fitting them with Gaussian profiles using the procedure implemented in the DECH software by Galazutdinov (2007). As a result of our study of the interstellar line profiles, three main absorption components, with the heliocentric radial velocities $V_r = -1$, -13 and -26 km s^{-1} (or, $+14$ km s^{-1}, $+2$ km s^{-1} and -11 km s^{-1} with respect to the LSR) were revealed.

These components were identified with three interstellar gas and dust complexes along the line of sight to Cyg X-1 up to its distance of 1.8 kpc by comparison to the 3D distribution of obscuring interstellar dust constructed by Lucke (1978). The nearest gas and dust complex is located at about 300 pc from the Sun and apparently is associated with the third absorption component ($V_{LSR} = -11$ km s^{-1}). The second complex, the largest one, which has the highest density and produces the strongest central absorption component ($V_{LSR} = +2$ km s^{-1}), is the Great Rift dissecting the Milky Way (located at distances of $800 - 1300$ pc). Associated with the third complex is the Cygnus star formation region which contains Cyg OB associations including Cyg OB3 where Cyg X-1 is located (≥ 1500 pc). Most probably, this complex produces the first absorption component with $V_{LSR} = +14$ km s^{-1}.

Besides, a weak component with $V_r = -43$ km s^{-1} ($V_{LSR} \simeq 30$ km s^{-1}) is seen in the strongest line profiles. The procedure applied to resolve components helped us to reveal this fourth component with certainty. Most probably, it is associated with the approaching wall of the expanding interstellar envelope around the Cyg OB3 association (superbubble). The component of this envelope that moves away was not revealed. This is an argument for Cyg X-1 being localized within the Cyg OB3 association. According to our data, this wall has higher ionization than the other three gas and dust complexes.

Using the equivalent widths of interstellar lines (Table 2), we determined the abundance of interstellar calcium, averaged along the line of sight to Cyg X-1, and found $[N(\mathrm{Ca})/N(\mathrm{H})]_{ISM} = 6 \cdot 10^{-10}$. Interstellar Ca depletion is typical of interstellar matter in our Galaxy, $[\mathrm{Ca/H}]_{ISM}/[\mathrm{Ca/H}]_{\odot} = 3 \cdot 10^{-4}$. The ionization degree is $N(\mathrm{Ca\,II})/N(\mathrm{Ca}) = 0.974$.

Thus, our study of the interstellar line profiles allows us to find the distribution of interstellar matter along the way to Cyg X-1. The obtained pattern of this distribution is an extra argument in favor of Cyg X-1 being localized in the Cyg OB3 association, at a distance of 1.8 kpc from the Sun. Other arguments are the coincidence of their localization in the sky, proper motions, independently obtained distances. The difference in their radial velocities is found to be less than the velocity dispersion of Cyg OB3 stars, 9.5 km s^{-1}. Consequently, the X-ray binary Cyg X-1 seems to have been born in this association. The upper limit on

the peculiar velocity of this object received as a result of the SN explosion (kick effect) is about 16 $\mathrm{km\,s^{-1}}$.

ACKNOWLEDGMENTS. This study was supported by the Russian Foundation for Basic Research through grants 12-02-01237-a and 12-02-97006-a. We thank Prof. A. S. Rastorguev and A. M. Melnik for discussion.

REFERENCES

Aab O. E. 1983, Soviet Astron. Letters, 9, 315

Abubekerov M. A., Antokhina E. A., Cherepashchuk A. M. 2004, Astron. Rep., 48, 550

Bochkarev N. G., Karitskaya E. A. 2007, in *Astrophysics and Cosmology after Gamow: Theory and Observations*, eds. G. S. Bisnovaty-Kogan et al., Cambridge Scientific Publishers, p. 371

Bochkarev N. G., Sitnik T. G. 1985, Ap&SS, 108, 237

Brand P.W.J.L., Zealey W. J. 1975, A&A, 38, 363

Galazutdinov G. 2007, http://www.gazinur.com/DECH-software.html

Karitskaya E .A. 2003, Kinematika i Fizika Nebesnykh Tel. Suppl., Kiev, No. 4, 230

Karitskaya E. A., Bochkarev N. G., Bondar' A. V. et al. 2008, Astron. Rep., 52, 362

Karitskaya E. A., Lyuty V. M., Bochkarev N. G. et al. 2006, IBVS, No. 5678, 1

Lucke P. B. 1978, A&A, 64, 367

Melnik A. M., Dambis A. K. 2009, MNRAS, 400, 518

Panchuk V., Klochkova V., Yushkin M., Najdenov I. 2007, in *The UV Universe: Stars from Birth to Death* (Proc. JD No. 4, IAU General Assembly, 2006), eds. A. I. Gomez de Castro & M. A.Barstow, Editorial Complutense, Madrid, p. 179

Panchuk V. E., Klochkova V. G., Yushkin M. V., Naidenov I. D. 2009, Journal of Optical Technology, 76, 42

Reid M. J., McClintock J. E., Narayan R. et al. 2011, ApJ, 742, 83

Walborn N. R. 1973, ApJ, 179, L123

Yushkin M. V., Klochkova V. G. 2005, Preprint of the Special Astrophysical Observatory No. 206

Zabolotskikh M. V., Rastorguev A. S., Dambis A. K. 2002, Astron. Lett., 28, 454

Ziolkowski J. 2005, MNRAS, 358, 851